

In-situ tuned photoelectric properties of PtS₂ transistor

Yana Cui¹, Wentao Gong¹, Gang Zhao¹ and Weike Wang^{1a)}

¹ *Synergetic Innovation Center for Quantum Effects and Application, Key Laboratory of Low-dimensional Quantum Structures and Quantum Control of Ministry of Education, College of Physics and Electronics Science, Hunan Normal University, Changsha, 410081, Hunan, China*

PACS:

Keywords: Photoelectric properties, Strain, PtS₂, Transistor.

a) To whom correspondence should be addressed. E-mail: wkwang@hunnu.edu.cn
or yanacui@hunnu.edu.cn

Abstract

Strain engineering is a powerful and widely used strategy for boosting the performance of electronic and optoelectronic devices. Here, we demonstrate an approach to tune the photoelectric properties of Platinum sulfide (PtS₂) by using a ferroelectric substrate PMN-PT as the strain generator. It is found that both the drain current and responsivity of the PtS₂ photodetector is directly coupled to the electrostriction of PMN-PT, showing a high strain-tuned ratio $\sim 10^3$, high responsivity up to 6.3×10^3 A/W and detectivity of 9.3×10^{12} Jones. Additionally, a high photogain $\approx 5 \times 10^5$ is obtained at a gate voltage $V_g = 15$ V. Our results provide an effective method for manipulating electrical properties and optimizing performance of two dimensional layered (2D) materials based optoelectronic devices.

Introduction

The layered two-dimensional material has attracted more and more attention in recent years because of its physical properties and promising potential applications in the field of field-effect transistors, optoelectronics devices, thermoelectric devices and so on¹⁻⁴. Among them, many 2D semiconductor photodetectors have been demonstrated with excellent performance. For example, Ta₂NiSe₅ photodetector attains ultrahigh photoresponsivity up to 17.21 A / W⁵, and GeP phototransistor achieves highly anisotropic photoresponsivity⁶. It is well known that the transistor performance was largely depredated due to scattering from charged surface states and impurities, surface roughness and so on. Thus, it improves the performance of transistors through external physical methods, for instance, by decorating Au nanoparticles on the surface, MoS₂ phototransistor exhibits a threefold enhancement in the photocurrent⁷. The PtS₂ phototransistor on h-BN substrates shows a sharply increasing responsivity⁸. Usually strain can effectively tune the physical properties of the material, by applying a strain through lattice mismatch between epitaxial films and substrates or through bending of films on elastic substrates. Applying strain can be used to constructe an in-situ controlled photodetector, which will benefit to designing and optimizing the performance of 2D photodetectors in practical applications.

Recently, as one of the tenth transition metal dichalcogenide, PtS₂, has attracted the attention of many scientists due to its high mobility and air stability¹⁰⁻¹⁴. Interestingly, PtS₂ shows a layer-dependent band gap from 1.6 eV of monolayer to 0.25 eV of bulk¹⁵. Moreover, theoretical calculations have demonstrated that the band gap of PtS₂ can be finely modulated under mechanical strain^{16,17}. In experimental, Yuan et al. explored photoelectric performance of PtS₂ under pressure study, showing the pressure-enhanced photocurrent¹⁸. Those research results indicate the possibility of modulating photoelectric properties of PtS₂ by means of applying strains. The relaxation type ferroelectric single crystal 0.72PbMg_{1/3}Nb_{2/3}O₃-0.28PbTiO₃ (PMN-PT) has a high piezoelectric constant and relatively high piezoelectric activity^{19,20}, and can serve as strain generator controlled by the external electric field²¹. In this work, we

employed piezoelectric materials PMN-PT as the strain generator. By mounting an PtS₂ ultrathin flake onto the PMN-PT substrate, we demonstrated that the drain current is directly tuned by the electrostriction of PMN-PT. The in-situ strains are finely manipulated by an external electrical field. We systematically studied the photoelectric performance of the device on PMN-PT substrate. The responsivity can be tuned up to 6.3×10^3 A / W. Using strain-engineered 2D materials with ferroelectrics represents a fundamentally exciting platform to explore the wide variety of other electric-field-tuned photoelectronic properties in the 2D materials world.

In order to study the strain effect on electron transport properties of PtS₂, we exfoliated bulk PtS₂ to obtain ultrathin flakes by scotch-tape based micromechanical exfoliation method, and transferred onto monocrystal PMN-PT substrate with (001) orientation and the thickness of 0.5 mm. The PtS₂ device was fabricated by standard electron beam lithography (EBL), and Ti / Au (10 nm / 80 nm) was deposited as the contact electrode. The schematic diagram of the device is illustrated in figure 1(a). The PtS₂ device consists of four electrodes, in which two electrodes were not contacted to the sample acted as Gate Electrodes, and the others were the source-drain electrodes. Figure 1 (b) shows an atomic force microscope image of a typical PtS₂ device. The thickness of the sample is about 36 nm in figure 1 (c). The Raman spectrums of PtS₂ measured on PMN-PT and on SiO₂ / Si substrates as shown in figure 1 (d). The observed Raman peaks agrees with reported results⁸, showing that the sample is intact and not damaged.

Results and discussion

Firstly, we performed electronic transport measurements in dark conditions. The electrical characterization of the PtS₂ transistor was performed using a semiconductor characterization system (4200SCS, Keithley) with a probe station (CRX-6.5K, Lake Shore). Figure 2 (a) displays the output characteristics $I_{ds}-V_{ds}$ of the PtS₂ device under different gate voltages (V_g). All $I_{ds}-V_{ds}$ characteristics show linear behavior in the region of approximately zero voltage, indicating that the Ti / Au electrode has good ohmic contact with the PtS₂ flake. In addition, the $I_{ds}-V_{ds}$ curve strongly depends on gate voltage (V_g), that is, the slope of the $I_{ds}-V_{ds}$ curve increases as V_g increases,

showing the strain-dependent conductance characteristics. We also measured the source-drain current as a function of the gate voltage measured at room temperature with $V_{ds} = 1$ V, as shown in figure 2 (b). The I_{ds} increases from 0.1 nA to 0.33 μ A with increase of the gate voltage V_g , leading to a high strain-tuned ratio $\sim 10^3$. Note that the above device characteristic for I_{ds} - V_g was obtained multiple times by cycling back and forth between “on” and “off” to ensure that the observed effects were reproducible and reversible. In our case, the gate voltage is applying across the PtS₂ channel, thus, we can reasonably ignore the ferroelectric polarization related charge transfer. According to the piezoelectric constant of the substrate ($d_{33} \approx 730$ pm / V), it can be judged that the compressive stress of the sample is about 0.7 % with $V_g = 10$ V²². The corresponding electric field induced a considerable strain due to electrostriction of PMN-PT can effectively pass on the PtS₂ flake owing to fine adsorption between flake and substrate. Thus, the band gap of the PtS₂ flake becomes narrow due to the PtS₂ flake compressed²³, and the carrier concentration in the conductive channel increases. The gate voltage increases, and the I_{ds} rapidly raised. Those measurement results agree well with the result of theoretical prediction, clearly showing tunable electronic transport properties of PtS₂ by strain.

Then, we checked the optoelectronic properties of PtS₂ with remaining strain constant and all the measurements were carried out under five gate voltage. Figure 3 summarizes the optoelectronic properties of the PtS₂ device with $V_g = 5$ V under $\lambda = 445$ nm laser illumination. As is shown in figure 3 (a), the comparison of the output characteristics I_{ds} - V_{ds} of PtS₂ under dark field and the laser irradiation clearly manifest the a net increase in the current. For further study, we measured the time-dependent photoresponse with different irradiation power intensities. Figure 3 (b) shows the I - T curves at different laser power intensities, one can clearly see that the I_{ds} gradually increases with increasing power intensity. The photoresponsivity (R) is one of the most important figures of merit to evaluate the sensitivity of a photodetector. R can be determined as, $R = I_{ph} / PS$ ²⁴, where I_{ph} is the photogenerated current, P is the power intensity and S is the effective irradiated area on the device. The calculated responsivity of the device is shown in figure 3 (c). From which, we can see that the

responsivity achieves 4.45×10^2 A / W at a power intensity of 11.38 mW / cm² and decreases with increasing power intensity. The decrease in photoresponsivity at higher illumination intensities is due to trap states present inside PtS₂ or at the interface between PtS₂ and substrate^{25,26}. Figure 3 (d) displays the cyclability of the PtS₂ device under power intensity of 21.83 mW / cm² by intentionally switching on / off the incident light, which clearly shows the stability of the on-off switching behavior. In the inset of figure 3 (d), one can see that the response time of the device is very short, that is, the rise time and fall time are 0.44 s and 0.42 s respectively. The switching speed is comparable or faster than many other reported 2D photoelectronic devices^{27,28}. Noticed that those results are roughly in accordance with the previous reported⁸, which is in favor of further study on strain effects.

For the further investigation of strain-tuned photoelectronic properties of the PtS₂ device, we performed systematical measurements on photocurrent as a function of power intensity and gate voltages. Figure 4 summarizes optoelectronic properties of PtS₂ device under electrical field induced strains. The relationships between the gate voltage V_g and source-drains current I_{ds} of the device at different illumination intensities are depicted in figure 4 (a). With increasing V_g from 0 to 10 V, the substrate shrinks, corresponding to the compressed strains, and the I_{ds} of the device sharply raised up, then approached a saturation current. However, upon V_g decreasing from 0 to -5 V, the substrate expands, corresponding to the tensile strain, and the I_{ds} rapidly reduced to the saturation value. The three-dimensional schematic diagram of the photocurrent is plotted in figure 4 (b). It is clearly seen that the evolution of the photocurrent with the gate voltage V_g and the laser power, which exactly demonstrates the strain modulated optoelectrical properties of PtS₂. In our few-layered PtS₂ photodetector, changes in transport and photodetection behaviors with strain may arise from the piezoresistive effect, where strain results in changes in band gap structure and density of states of the carriers. When $V_g > 0$ V, a compressive strain is applied, the band gap becomes smaller²⁵. With the decrease of the band gap, the absorption of photons with energy higher than the bandgap ($E_{ph} > E_{bg}$) can generate more free carriers, resulting in a net increase in the current.

Other figures of merit important to a photodetector, such as photoresponsivity, photogain, and detectivity, can also be modulated and largely enhanced by strain. We then study the photoresponsivity and detectivity of the device with strain, which is shown in figure 4 (c). It can be seen that the responsivity increases with increasing V_g , for $V_g = 15$ V, the responsivity of the photodetector can reach up to 6.3×10^3 A / W, such value is two times higher than the previous reported⁸. Detectivity (D^*) usually can be defined as $D^* = R_\lambda S^{1/2} / (2eI_{dark})^{1/2}$, is another critical parameter to evaluate the detection performance of photodetectors. It can see that detectivity reaches 9.3×10^{12} Jones at $V_g = 2$ V for our device, which is 30 times higher than the previous reported (2.9×10^{11} Jones)⁸. The photogain (G) is defined as the ratio between the number of electrons collected and the number of absorbed photons in the device per unit time. Figure 4d shows photogain of the device derived from data in figure 4b according to $G = [I_{ph}/(\eta P)](h\nu/q)$, where η is the absorption of few-layered PtS₂, h is Planck's constant, q is the electronic charge, and ν is the frequency of incident light. where η is the absorption of few-layered PtS₂, $h\nu$ is the photon energy. Figure 4d shows that G increases with decreasing excitation laser power and reaches $\approx 5 \times 10^5$ when the excitation laser intensity is 14.83 mW / cm², if 4% absorption is estimated. These results suggest that strain is able to function as a controlling gate signal and effectively modulates the photodetection properties of few-layered PtS₂ optoelectronic device.

Conclusion

To summarize, we have successfully fabricated few-layered PtS₂ phototransistors on a PMN-PT substrate and studied photoelectric properties of PtS₂ under strain control. The responsivity of this phototransistor is 6.3×10^3 A / W, and its strain-tuned ratio is $\sim 10^3$. A maximum detectivity of 9.3×10^{12} Jones with a 30-fold improvement over the reported highest photoresponsivity for few-layered PtS₂ phototransistors is demonstrated under strain. In addition, under compressive strain state at $V_g = 15$ V, an ultrahigh photogain up to 5×10^5 is achieved. Therefore, PtS₂ will have unique advantages in the future photoelectric field due to its outstanding optoelectronic performance and the strain tuned photocurrent. Based on our results,

incorporating strain engineering into future TMD devices occurs highly promising to tune the material properties of this class of two-dimensional materials.

Acknowledgments

This work was financially supported by the National Natural Science Foundation of China, Grant No.11604340, No. 11304321, and No. 11574081; and the project funded by China Postdoctoral Science Foundation, Grant No. 2015LH0018 and No. 2017M610474.

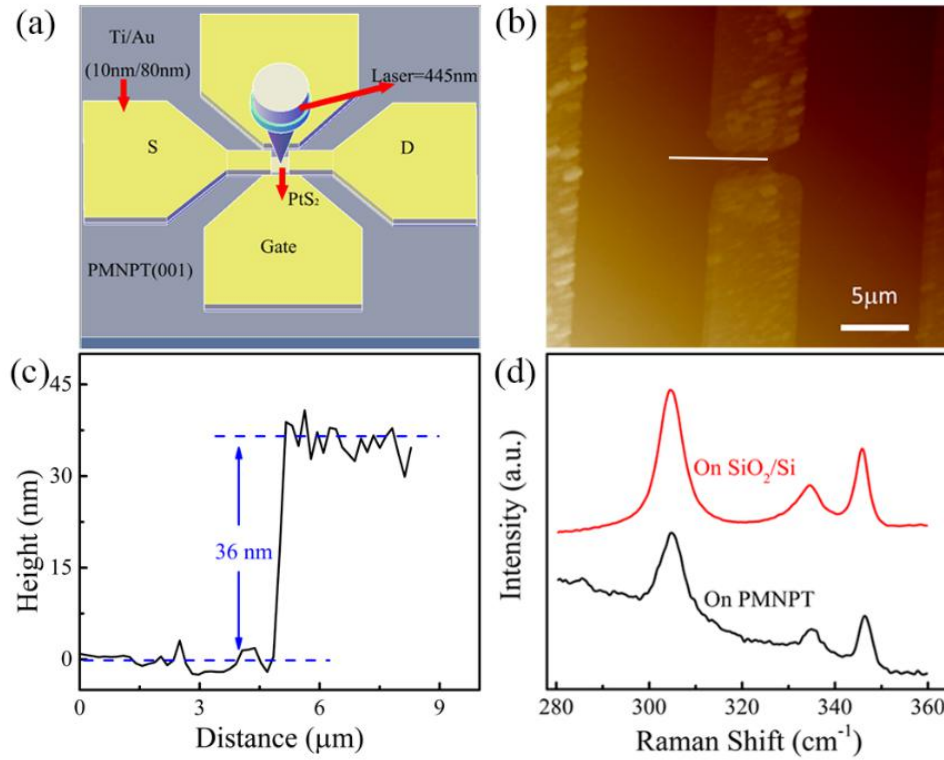


Figure 1. (a) Schematic structure of the fabricated PtS₂ device. (b) The atomic force microscope (AFM) image of a typical fabricated device. (c) The height profile along the white line of figure 1 (b) is shown here, and the thickness is about 36 nm. (d) Raman spectrum of PtS₂ on PMN-PT and on Si / SiO₂.

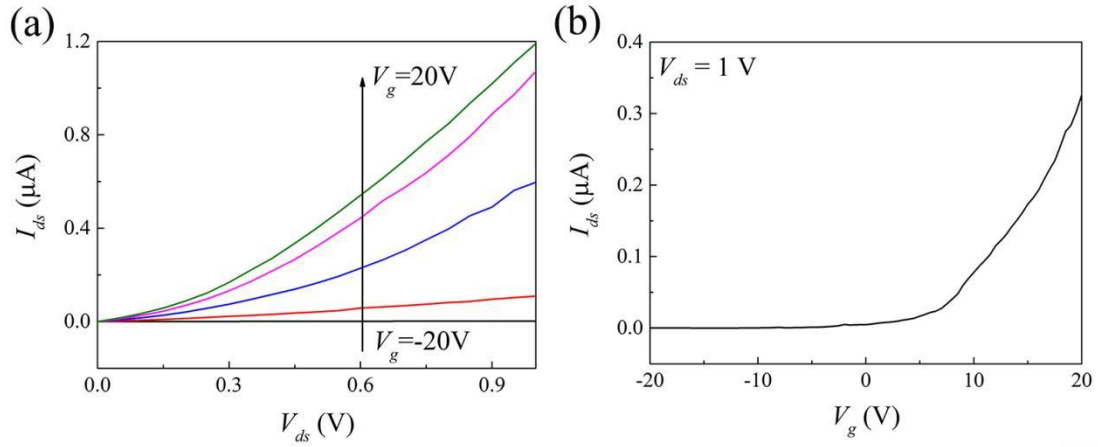


Figure 2. In the dark, the electronic transport properties of few-layered of PtS₂ based on PMN-PT. (a) Output characteristics I_{ds} - V_{ds} of the device at different back-gate voltages. (b) Transfer curves I_{ds} - V_g of the device with V_g from -20 to 20 V at the drain-source bias $V_{ds} = 1\text{ V}$.

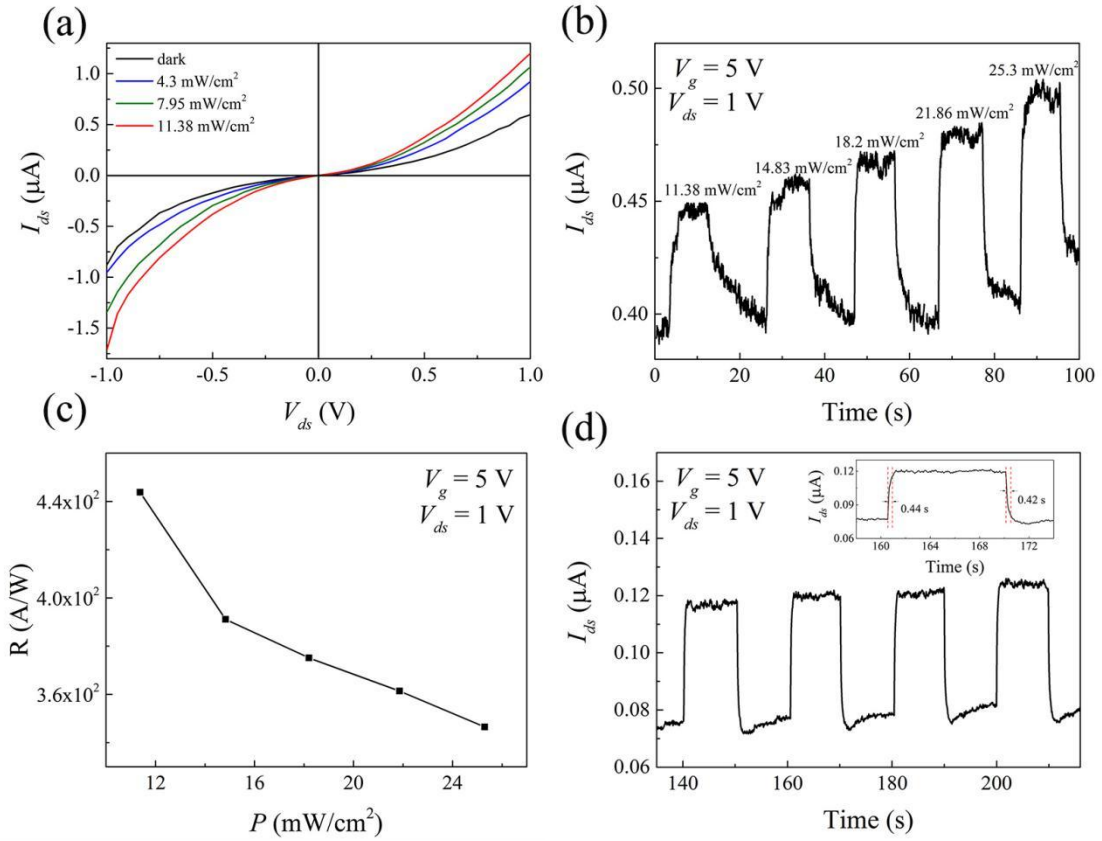


Figure 3. The photoelectric properties of few-layered of PtS₂ based on PMN-PT when $V_g = 5$ V is applied ($\lambda = 445$ nm). (a) The output curves (I_{ds} - V_{ds}) of the phototransistor recorded in the dark and under different illumination intensities. (b) Light intensity-dependent photoresponse at $V_{bias} = 1$ V. (c) The responsivity as a function of laser power intensity. (d) Timereolved photoresponse recorded at $V_g = 5$ V and $V_{ds} = 1$ V, inset: response rate of photodetector acquired from one magnified circle of response with rising time 0.44 s and decay time 0.42 s.

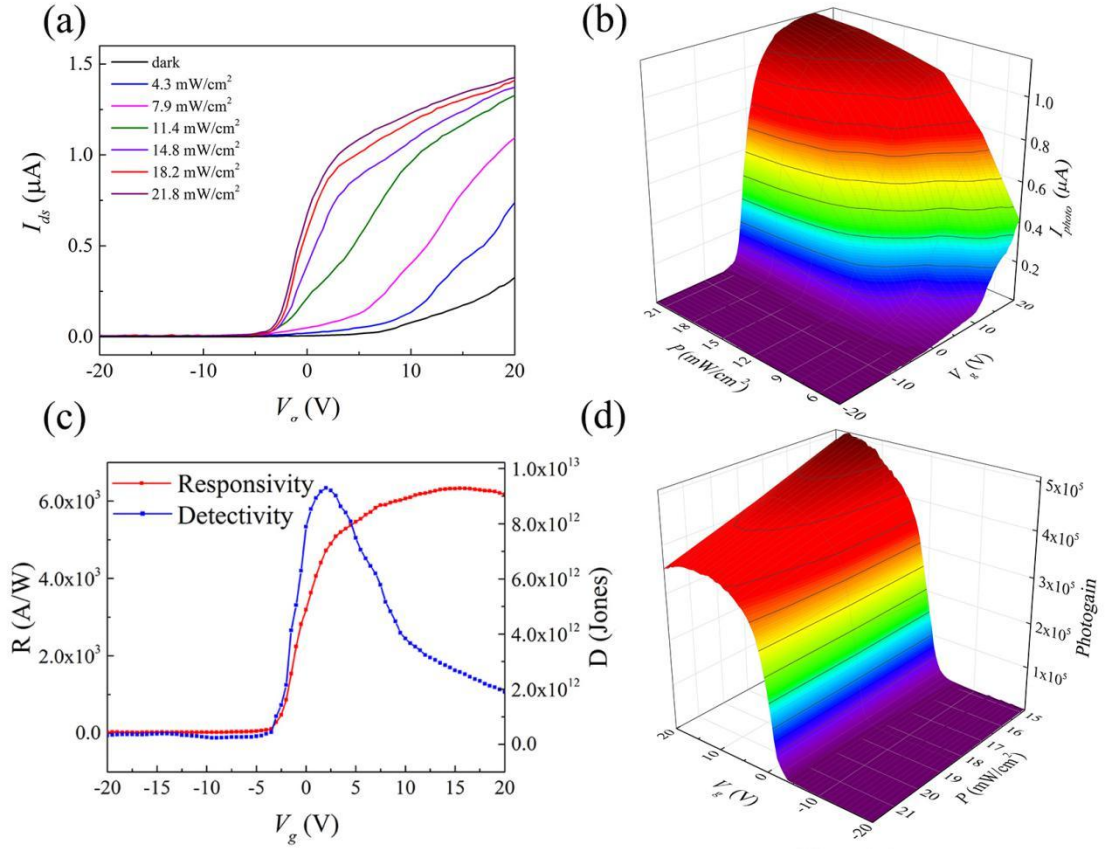


Figure 4. (a) Transfer curves of the device recorded in the dark and under different illumination intensities at $V_{ds} = 1$ V. (b) 3D view of photocurrent mapping. (c) The responsivity and detectivity as a function of V_g measured at $V_{ds} = 1$ V. (d) 3D view of photogain mapping at $V_{ds} = 1$ V.

References:

- 1 S. Z. Butler, S. M. Hollen, L.Y. Cao *et al.*, “Progress, challenges, and opportunities in two-dimensional materials beyond graphene,” ACS Nano **7**, 2898-2926 (2013).
- 2 T. Mueller, F. Xia and P. Avouris, “Graphene photodetectors for high-speed optical communications,” Nature Photon. **4**, 297-301 (2010).
- 3 W. K. Wang, L. Li, Z. T. Zhang *et al.*, “Ultrathin GaGeTe p-type transistors,” Appl. Phys. Lett. **111**, 203504 (2017).
- 4 Y. Lee, J. Kwon, E. Hwang *et al.*, “High-performance perovskite-graphene hybrid photodetector,” Adv. Mater. **27**, 41-46 (2015).
- 5 L. Li, W. K. Wang, L. Gan *et al.*, “Ternary Ta₂NiSe₅ flakes for a high-performance infrared photodetector,” Adv. Funct. Mater. **26**, 8281-8289 (2016).
- 6 L. Li, W. K. Wang, P. L. Gong *et al.*, “2D GeP: an unexploited low-symmetry semiconductor with strong in-plane anisotropy,” Adv. Mater. **30**, 1706771 (2018).
- 7 J. S. Miao, W. D. Hu, Y. L. Jing *et al.*, “Surface plasmon-enhanced photodetection in few layer MoS₂ phototransistors with Au nanostructure arrays,” Small **11**, 2392-2398 (2015).
- 8 L. Li, W. K. Wang, Y. Chai *et al.*, “Few-layered PtS₂ phototransistor on h-BN with high gain,” Adv. Funct. Mater. **27**, 1701011 (2017).
- 9 K. Kaasbjerg, K. S. Thygesen, and A-P. Jauho, “Acoustic phonon limited mobility in two-dimensional semiconductors: deformation potential and piezoelectric scattering in monolayer MoS₂ from first principles,” Phys. Rev. B **87**, 235312 (2013).
- 10 W. X. Zhang, Z. S. Huang, W. L. Zhang *et al.*, “Two-dimensional semiconductors with possible high room temperature mobility,” Nano Res. **7**, 1731-1737 (2014).
- 11 Z. S. Huang, W. X. Zhang, and W. L. Zhang “Computational search for two-dimensional MX₂ semiconductors with possible high electron mobility at room temperature,” Materials **9**, 716 (2016).
- 12 Z. G. Wang, Q. Li, F. Besenbacher *et al.*, “Facile synthesis of single crystal PtSe₂ nanosheets for nanoscale electronics,” Adv. Mater. **28**, 10224-10229 (2016).
- 13 C. Yim, K. Lee, N. McEvoy *et al.*, “High-performance hybrid electronic devices from layered PtSe₂ films grown at low temperature,” ACS Nano **10**, 9550–9558 (2016).

- 14 Y. D. Zhao, J. S. Qiao, Z. H. Yu *et al.*, “High-electron-mobility and air-stable 2D layered PtSe₂ FETs,” *Adv. Mater.* **29**, 1604230 (2016).
- 15 Y. D. Zhao, J. S. Qiao, P. Yu *et al.*, “Extraordinarily strong interlayer interaction in 2D layered PtS₂,” *Adv. Mater.* **28**, 2399-2407 (2016).
- 16 P. Miró, M. Ghorbani-Asl and T. Heine, “Two dimensional materials beyond MoS₂: noble-transition-metal dichalcogenides,” *Angew. Chem. Int. Ed.* **53**, 3015-3018 (2014).
- 17 P. Johari and V. B. Shenoy, “Tuning the electronic properties of semiconducting transition metal dichalcogenides by applying mechanical strains,” *ACS Nano* **6**, 5449-5456 (2012).
- 18 Y. F. Yuan, Z. T. Zhang, W. K. Wang *et al.*, “Pressure-induced enhancement of optoelectronic properties in PtS₂,” *Chinese Phys. B* **27**, 347-351 (2018).
- 19 L. E. Cross, S. J. Jang, R. E. Newnham *et al.*, “Large electrostrictive effects in relaxor ferroelectrics,” *Ferroelectrics* **23**, 187-191(1980).
- 20 S. L. Swartz, T. R. Shrout, W. A. Schulze *et al.*, “Dielectric properties of lead-magnesium niobate ceramics,” *J. Am. Ceram. Soc.* **67**, 311-314 (1984).
- 21 W. H. Hou, A. Azizimanesh, A. Sewaket *et al.*, “Strain-based room-temperature non-volatile MoTe₂ ferroelectric phase change transistor,” *Nature Nanotechnology* **14**, 668-673 (2019).
- 22 J. F. Wang, D. Cao, Y. Zhou *et al.*, “Effects of residual and tunable strain on the transport properties and electroresistance effects in thin films of La_{0.39}Pr_{0.24}Ca_{0.37}MnO₃,” *J. Alloys Compd.* **649**, 819-823 (2015).
- 23 S. Ahmad, “Strain and electric field dependent variation in electronic and thermoelectric properties of PtS₂,” *Results Phys.* **17**, 103088 (2020).
- 24 Q. Guo, A. Pospischil, M. Bhuiyan *et al.*, “Black phosphorus mid-infrared photodetectors with high gain,” *Nano Lett.* **16**, 4648 (2016).
- 25 O. Lopez-Sanchez, D. Lembke, M. Kayci *et al.*, “Ultrasensitive photodetectors based on monolayer MoS₂,” *Nature Nanotech.* **8**, 497-501 (2013).
- 26 S. Ghatak, A. Pal and A. Ghosh, “Nature of electronic states in atomically thin MoS₂ field-effect transistors,” *ACS Nano* **5**, 7707–7712 (2011).
- 27 M. Hafeez, L. Gan, H. Q. Li *et al.*, “Chemical vapor deposition synthesis of

ultrathin hexagonal ReSe₂ flakes for anisotropic Raman property and optoelectronic Application,” *Advanced Materials* **28**, 8296-8301 (2016).

28 M. M. Furchi, D. K. Polyushkin, A. Pospischil *et al.*, “Mechanisms of photoconductivity in atomically thin MoS₂,” *Nano Letters* **14**, 6165-6170 (2014).